Korean J. Chem. Eng., 33(5), 1612-1619 (2016)
DOI: 10.1007/s11814-016-0024-7

pISSN: 0256-1115
eISSN: 1975-7220

Flash spray characteristics of a coal-liquid carbon dioxide slurry

Kangwook Kim, Hakduck Kim, Changyeon Kim, and Juhun Song†

School of Mechanical Engineering, Pusan National University, Busan 46241, Korea
(*Received 8 September 2015 • accepted 25 January 2016*)

Abstract−Liquid carbon dioxide (LCO_2) could potentially be utilized in coal gasification plants for effectively transporting coal particles, replacing conventional carriers such as water (H_2O), particularly in wet-fed gasifiers. However, it is essential to understand the atomization behavior of LCO_2 leaving an injector nozzle under both coal-free and coal-fed conditions. We examined the atomization behavior of a coal-LCO_2 slurry during the throttling process. The injector nozzle was mounted downstream of a high-pressure spray system. The effect of upstream pressure on flash atomization and devolatilization behavior was presented. Compared with the coal-LCO_2 mixture, the spray pattern of the coal-water mixture was significantly different, since it evidenced a Rayleigh-type breakup mode. This difference indicates that the coal-water slurry did not transport the coal as effectively as the coal-LCO_2 slurry.

Keywords: Coal Gasification, Flashing Spray, Liquid Carbon Dioxide (LCO_2), Coal Slurry, Devolatilization

INTRODUCTION

Coal gasifiers could potentially utilize abundant coal worldwide for the production of either electricity or high-quality synthetic fuel. Although this process may produce less greenhouse emissions than conventional coal-fired power plants, it has been observed that existing gasifiers with slurry feeding, i.e., using water (H_2O) as the transport medium to deliver coal, exhibit diminished performance, particularly when low-rank coal (LRC) is used. Unless a drying unit is installed separately, the excess H_2O content in LRC reduces the portion of coal in the mixture, and therefore the amount of synthetic gas converted from the coal. To solve this problem, it is desirable to develop a new coal supply technology, in which slurry mixtures of pressurized liquid carbon dioxide (LCO_2) and LRC are delivered. The LCO_2 is used to transport coal in a more efficient manner, as compared with conventional carriers such as H_2O. This may provide another route for utilizing CO_2 emissions in the coal gasification sector. To implement this technology, it is essential to understand the hydraulic and spray characteristics of slurry mixtures at different operating conditions, such as pressure, temperature, and flow velocity.

It has been suggested that coal feeding with LCO_2 could increase the blending ratio of coal in the transport medium as compared with its transport with H_2O [1-3]. This would be very useful when LRC with high moisture content near the coal surface, or through the entire coal volume, is used. The increased blending ratio is attributable to the combined effects of the lower viscosity and better wettability of LCO_2 with the internal and external surfaces of the coal. This enhanced adsorption of LCO_2 into the coal definitely prevents water from reentering the coal pores. This behavior is demonstrated in the LICADO process, where mineral and water content is separated from the coal-LCO_2 slurry [1].

Meanwhile, compressed LCO_2 has a different impact on the atomization and subsequent pyrolysis characteristics at the injector nozzle of slurry-fed gasifiers when LCO_2 slurry is sprayed. Compared to the conventional spray pattern of H_2O, LCO_2 produces effective breakup, leading to smaller liquid droplets, because of lower viscosity and higher momentum flux. This helps transport coal particles more uniformly inside the gasifier. This feature of better dispersion is more attractive since it requires less heat release from partial combustion and thus less oxygen supply to the coal gasifiers.

Application of LCO_2 to the impact cleaning of snow particles has been found in the literature [4]. In this process, CO_2 is expanded through a nozzle from a high pressure to an atmospheric pressure condition. The flash atomization and breakup mechanism of LCO_2 were examined using different liquid contents during the throttling process across the nozzle. At some condition, the LCO_2 experiences a sudden pressure drop below saturation pressure. LCO_2 with different levels of superheat was investigated to understand the characteristics of flashing spray and snow particle formation. Zeng and Lee developed an atomization model for sprays in flash boiling conditions, and found that such sprays atomized by bubble growth, resulted in a smaller droplet size than that generated using aerodynamic force alone [5]. Recently, the spray characteristics and particle size of CO_2 produced by flash boiling have been getting more and more attention. Liu et al. used the laser diffraction method and model validation to determine the particle size distribution of the spray [6]. Liquid droplets and solid particles with a size of a few microns were observed [7]. However, the behavior of coal transport by the atomization of LCO_2 has not been experimentally evaluated.

In other research, supercritical CO_2 was used to extract water from LRC and to prepare activated coals with a high surface area per volume [8-10]. This is known as the low-temperature drying process. The enhanced adsorption/desorption behavior of compressed CO_2 was used for other applications, such as incorporat-

†To whom correspondence should be addressed.
E-mail: jxs704@pusan.ac.kr

ing other low-molecular weight compounds (i.e., adhesives) into glassy polymers [11]. This effect is due to the high diffusivity, solubility, and plasticizing action of compressed CO_2 in polymers. When pressure is released, absorbed CO_2 rapidly diffuses from the polymer, while other bonding compounds desorb more slowly during the infusion process.

There are many reports on the atomization of coal-water slurry (CWS) that primarily focus on the atomizer performance and mean droplet diameter [12,13]. Furthermore, some morphology results for coaxial two-fluid air-blast atomization have been documented in the literature [14]. In particular, four different breakup modes were identified, depending on the magnitude of the co-flowing air velocity. When the viscosity of CWS is low, the CWS jet experiences a Rayleigh-type breakup at low air velocities. In contrast, the CWS jet undergoes a fiber-type breakup at high air velocities. When the air velocity is extremely high, the CWS jet is within the normal breakup region. Dechelette et al. studied the high-speed visualization of shear-thinning liquid jet breakup, which characterizes non-Newtonian liquid jet behavior [15,16].

In this study, the spray patterns of a coal-LCO_2 mixture were examined during the throttling process. The injector nozzle was mounted downstream of a high-pressure flashing spray system, while the downstream pressure was controlled by a back pressure regulator. A microscopic shadowgraph apparatus and gas analyzer were used to evaluate the flash atomization and devolatilization process presumably occurring during the throttling process.

EXPERIMENTAL SETUP

1. Flashing Spray Visualization System

Fig. 1 presents a schematic diagram of the high-pressure flashing spray system used in this study. It consisted of an upstream chamber (vessel), a middle block, and a downstream chamber (vessel). The middle block and two chambers had an optical quartz window to permit visualization of internal cavitation and flashing spray behavior during the throttling process. The window was designed to withstand pressures up to 100 bar at a peak temperature of 80 °C, and a pressure relief valve was installed to prevent pressure rises beyond this limit.

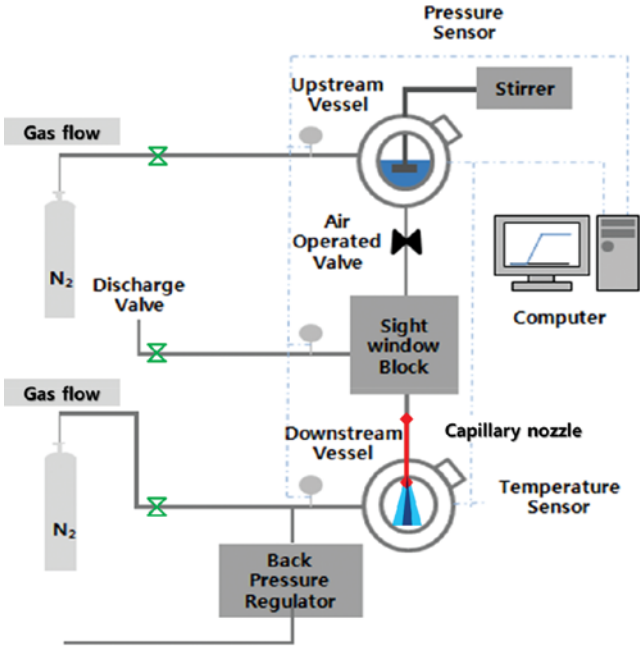

Fig. 1. Schematic of the experimental setup.

The saturated mixture of CO_2 was achieved by adjusting the temperature and mass of the solid CO_2 (SCO_2, dry ice). Different chamber temperatures were achieved with the use of a constant temperature bath. As seen in the figure, the nozzle was installed between the middle block and the downstream chamber. It was 300 mm long with an internal diameter of 0.4 mm. Two different materials are used for nozzles. Some are made of transparent Pyrex, so that the flow pattern inside the nozzle is visible. This is important for checking the capillary action in the low velocity condition and the cavitation phenomenon in the high velocity condition. However, a copper nozzle was used for this study. A data acquisition system was utilized to monitor the temperature and pressure inside each chamber, and a flow controller unit was used to turn the valves on and off pneumatically.

Three different phases of LCO_2 were prepared at a constant temperature by changing the pressures of the upstream and downstream chambers to 85/60, 75/50, and 65/40 bar. Nitrogen gas was used as filler when a pressure increase was required beyond the saturation pressure. The pressure difference between the two chambers was maintained constant at 25 bar. Fig. 2 illustrates how the three different initial states underwent different phase transitions, by employing the P-T diagram of CO_2. The pressure condition of 85/60 bar held the LCO_2 in the liquid phase during the throttling and subsequent spraying process. However, the LCO_2 experienced a phase transition from the liquid to the vapor phase at the condition of 65/40 bar. The constant pressure of the lower chamber was made possible by a backpressure regulator mounted downstream of the lower chamber. Otherwise, pressure in the lower chamber would have increased as the liquid flow filled the lower chamber, thereby compressing the gas. The dimensions of the high-pressure

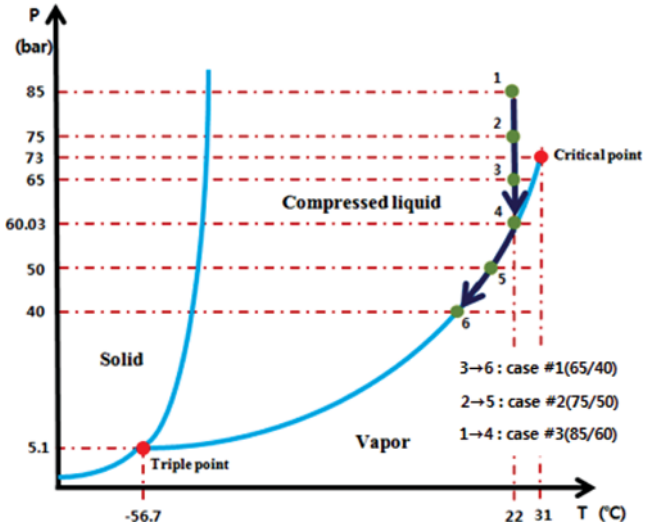

Fig. 2. Schematic of spray test condition mapping in the P-T diagram of CO_2.

Table 1. Dimensions of high-pressure flashing spray system

Parameters	Description
Chamber shape	Cylinder
Chamber diameter/length	5 cm/13.4 cm
Chamber volume	260 cm^3
Capillary nozzle inner diameter	0.4 mm
Capillary nozzle length	300 mm

flashing spray system are listed in Table 1. The diameter of optical window in the lower chamber is 5 cm providing the visualization region. It was desirable to fit most of spray penetration into this visualization region for all pressure conditions tested in this study. As a result, wetting of the chamber bottom by spray plume should be prevented. For this reason, we selected the nozzle with relatively high ratio of length to diameter as discussed earlier.

A shadowgraph technique was employed to examine the flashing spray patterns of the LCO_2 and its slurry with coal. During the throttling process across the nozzle, consecutive images were recorded at a frame rate of 1/40000 s using a high-speed camera. In the meantime, the pressure difference was also measured, to relate the spray patterns to the possibility of cavitation flow.

2. Coal Slurry Preparation and Characterization

The pulverized coal was weighed and mixed with the LCO_2 according to the appropriate blending ratio. The mixture was then poured into the upstream chamber. The magnetic stirring unit was mounted in the middle of the upstream chamber. It was operated under high-pressure conditions to provide better mixing and a more uniform dispersion of coal within the LCO_2 before the throttling and spray process occurred. The detailed properties of the coal are listed in Table 2. Adaro coal was used to prepare the coal slurries with LCO_2 and H_2O. The elemental composition and other components contained in the coal were analyzed (Table 2). The volatile content was 44.7 wt% on a mass basis, while the water and mineral content was 8.3 and 0.9 wt%, respectively. The blending ratio was 1.5% on a volume basis. The coal was pulverized to an average diameter of 45-75 μm. The gas composition of the coal slurry was measured after the throttling process. The coal sample was collected and analyzed to evaluate any changes in the morphology and surface structure of coal at different spray conditions.

Table 2. Properties of coal used in this experiment

Analysis	Contents	Values
Proximate analysis (wt%, wet basis)	Moisture	8.3
	Volatile matter	44.7
	Fixed carbon	46.1
	Ash	0.9
Ultimate analysis (wt%, dry ash free basis)	C	74.1
	H	5.9
	O	18.6
	N	1.3
	S	0.1
Density (kg/m^3)	1,100	

Table 3. Raw data of composition changes to calculate the coal conversion by using the ash-trace method

wt%	Raw coal	Coal sample after throttling process at 65/40 bar
Moisture	8.3	4.9
Volatile	44.7	54.4
Fixed carbon	46.1	34.3
Ash	0.9	6.4

The coal conversion was calculated by using the ash trace method and compositional changes during the throttling process (see Table 3). The ash fraction was measured between the initial coal and the coal sample after flash spraying by using a thermogravimetric analyzer (TGA). The ash content between the two samples was assumed to be constant when the initial amount of coal prior to the throttling process (m_o) was determined. The coal conversion (η) was calculated accordingly from the two ash fractions by Eq. (1):

$$\eta = \frac{m_o - m_t}{m_o} = 1 - \frac{m_t}{m_o} = 1 - \frac{\eta_{a,o}}{\eta_{a,t}} \quad (1)$$

where $\eta_{a,o}$ is the ash fraction of the initial coal sample, and $\eta_{a,t}$ is the ash fraction of the coal sample after experiencing the flashing spray.

RESULTS AND DISCUSSION

1. Spray Patterns of LCO_2

Fig. 3 gives the temporal variation of the differential pressure between the chambers during the throttling process. There is an abrupt change in the pressure decay, indicating the transition to expanding vapor flow inside the nozzle. This transition, due to bubble burst, is most noticeable during the throttling event encountered when pressure decreased from 65 to 40 bar. This condition produced a sudden pressure drop sufficiently below saturation pressure (~60 bar) at 22 °C inside the nozzle. During the decrease in CO_2 pressure, liquid droplets nucleated, which was accompa-

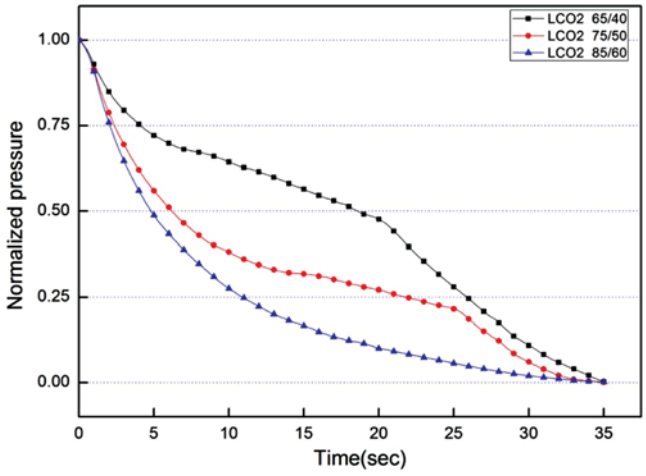

Fig. 3. Temporal variation of differential pressure between chambers during the throttling process.

nied by rapid liquid boiling into a gas bubble formation. In contrast, the LCO_2 from depressurizing from 85 to 60 bar experienced a continuous and smooth pressure decay during the throttling process. This indicates that this higher pressure level preserves the liquid phase inside the nozzle. In this experiment, the rate of pressure decay may closely relate to the flow rate within the nozzle. This observation is consistent with the results that vapor bubbles within the nozzle may cause a reduced mass flow of liquid by reducing the effective nozzle diameter [17]. For this reason, the drastic reduction of pressure decay may indicate the bubble formation that was observed especially for the pressure condition of 65/40 bar.

Fig. 4 shows spray patterns under different levels of upstream pressure (pressure difference), observed through a high-speed camera. There is a slight variation of spray pattern from one to other frame although it is steady state behavior. For better clarity, the image representing average characteristics was chosen in Fig. 4. As expected, the internal flashing from bubble formation in the condition of 65/40 bar caused a wider spray angle and shallower penetration length. This is sometimes called a "bowl spray." This represents a high level of flash-atomization, which is an effective breakup mechanism of the liquid column, due to a burst of bubbles. This results in a smaller droplet size. A similar phenomenon to the bowl spray pattern was observed with increasing degree of superheat in the modeling work of Senda et al. [18], and in the experimental work of Lin et al. [4]. As the degree of superheat increased, the breakup length became shorter, and the spray angle became larger. However, a spray angle reduction due to air entrainment occurred as the superheat was further increased [19]. Note that the experiment of Lin et al. [4] was conducted during a throttling process expanding to an atmospheric backpressure condition, which is different from the process used in the present work. The expansion to atmosphere was more suitable for the impact-cleaning process with LCO_2 and snow particle. In contrast, an expansion to higher downstream pressure (e.g., 40 bar) is more realistic to simulate the condition of coal gasification unit.

In contrast, a narrower spray angle and deeper penetration were observed during the flash boiling free condition of 85/60 bar. This is considered a normal jet spray. This difference is attributed to the higher velocity of the liquid flow inside the nozzle orifice. Fig. 5 depicts the dependence of the distribution of the atomized liquid size on the degree of flash boiling. A conventional image analysis technique was employed to obtain the particle size distribution. The results show that the mean diameter of the liquid spray was 130 μm for two spray conditions. However, the so-called normal

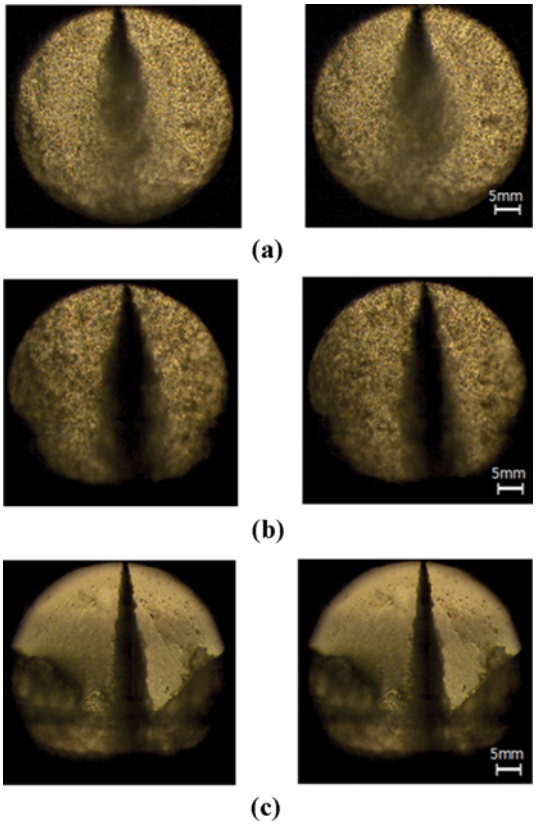

Fig. 4. Spray patterns under different levels of upstream pressure, observed through a high-speed camera: (a) 65/40 bar, (b) 75/50 bar, and (c) 85/60 bar.

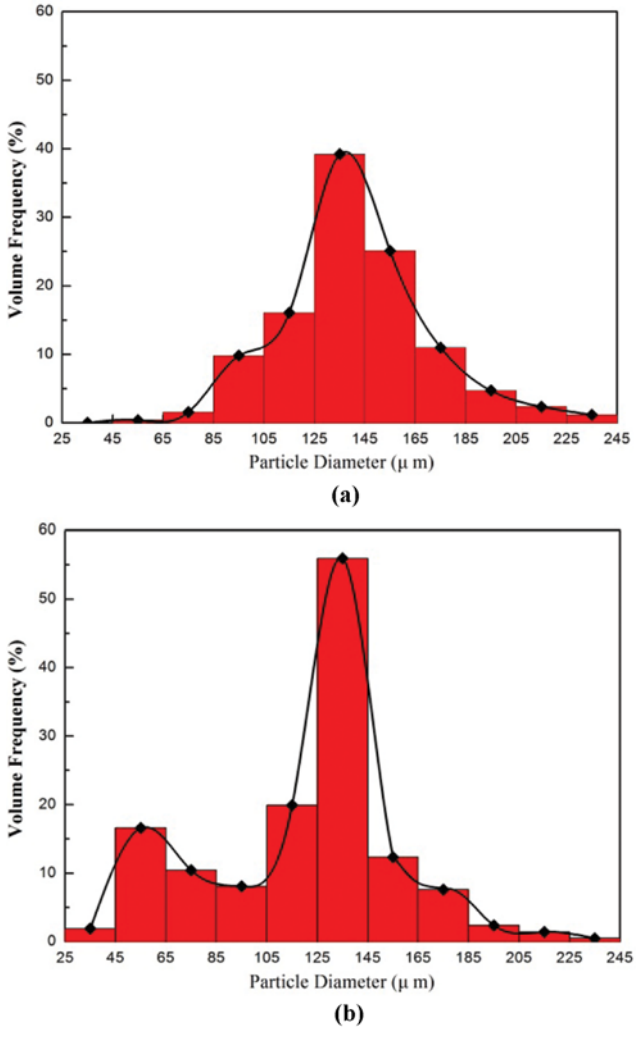

Fig. 5. Dependence of atomized liquid size distribution on degree of flash boiling: (a) 65/40 bar and (b) 85/60 bar.

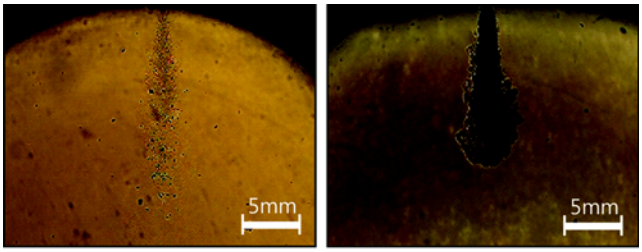

Fig. 6. Spray patterns of slurry mixtures of LCO_2 and coal at initial stage of spray development: (a) 65/40 bar and (b) 85/60 bar.

spray condition of 85/60 bar produced a greater deviation, as compared with the bowl spray condition of 65/40 bar. Other peaks appeared at low mean diameter ranging from 40-65 μm. The similar behavior of droplet size distribution was observed in both experiments of Lin's [4] and Xiao and coworkers [20]. For example, Xiao et al. demonstrated that the addition of CO_2 in the diesel spray produced much more uniform droplet size as a result of flash separation of CO_2 from the liquid.

2. Spray Patterns of Coal-LCO_2 Slurry

In this experiment, coal was first mixed with LCO_2 at a volume ratio of 1.5%. The slurry was ejected from the nozzle orifice. Fig. 6 presents the spray patterns of slurry mixtures of LCO_2 and coal at the initial stage of spray development. In the flashing spray condition of 65/40 bar, coal particles can be seen in most of the vapor flow in the shadow image. In contrast, the coal particles were transported inside dense liquid droplets in the non-flashing spray condition of 85/60 bar so that they were not seen. The higher velocity delivered the coal particles more uniformly into downstream of the chamber fitted with nozzle orifice. As gasification results are dependent on the mass transport rate and particle velocity, it is important to understand the fundamentals of slurry atomization [21,22].

Fig. 7 compares the gas composition of the LCO_2-coal slurry measured after the throttling process at two pressure conditions: (a) 65/40 and (b) 85/60 bar. During the gas sampling, the system was vented to the atmosphere and part of the ejected gas was fed to the gas analyzer. During gas sampling, oxygen concentration

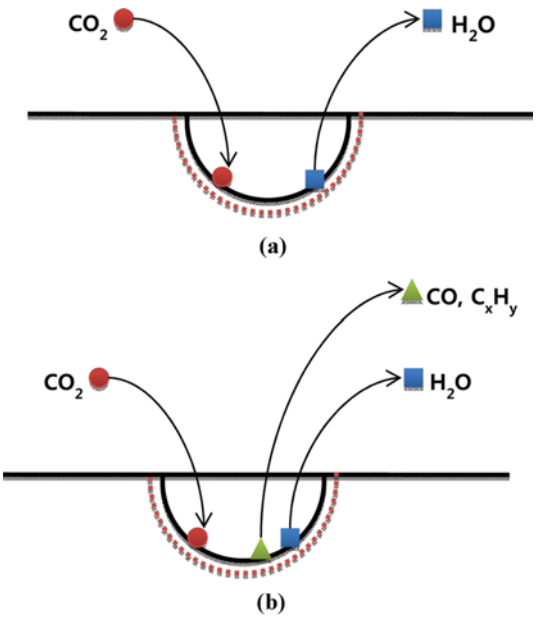

Fig. 8. Schematic diagram of (a) H_2O extraction process on the coal surface due to pore increase during a throttling process, and (b) H_2O and volatile extraction process on the coal surface due to pore increase and bonding weakening during the throttling process.

decreased from 21 to 0% and the CO_2 concentration increased. The CO and total hydrocarbon (C_xH_y) concentration increased to a certain level, even if small, during the flashing spray condition of 65/40 bar. However, a CO and C_xH_y concentration was not detected during the non-flashing spray condition. This difference indicates the possibility of flashing or destructive devolatilization processes of coal when the coal particles are sprayed under the LCO_2 vapor flow condition.

When internal flashing of LCO_2 occurs due to the pressure drop during the throttling process, coal particles may also be involved in the drastic pressure drop and thus produce light volatile products such as CO and H_2, or heavy hydrocarbons such as tar. Such gas releases seem to be more favorable when the surrounding is in the vapor phase, rather than in the liquid phase. Gas might be

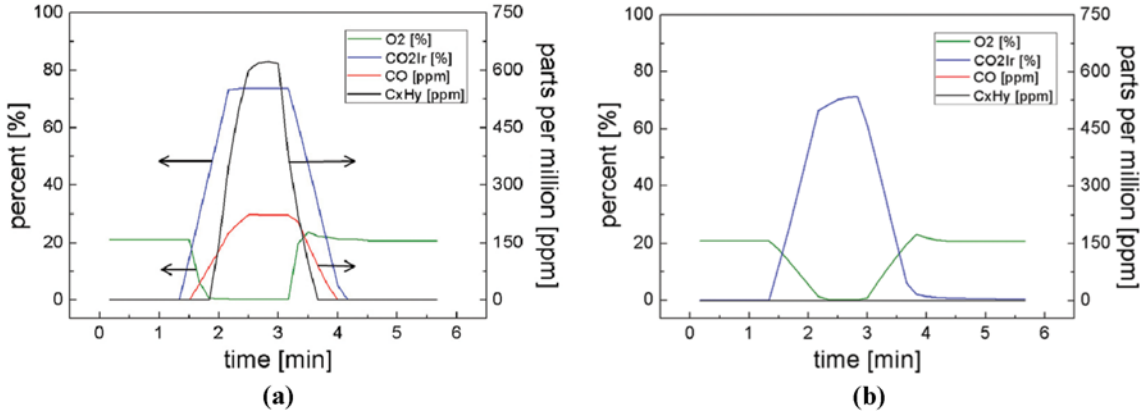

Fig. 7. Gas composition of LCO_2-coal slurry measured after throttling process: (a) 65/40 bar and (b) 85/60 bar.

transferred to the surroundings more rapidly by flash boiling vapor than by the liquid once the gas is released from the coal surface. The adsorbed CO_2 interacts with oxygen functional groups to weaken the hydrogen bonding among the coal macromolecules. This results in the release of volatile products, called flash devolatilization, when coal particles undergo a pressure drop.

As discussed in the introduction, supercritical CO_2 was used to extract water from LRC, which results in the production of a high surface area per volume. This mechanism was observed in the experiments of Iwai et al. [8,9], and is schematically illustrated in Fig. 8(a). The CO_2 released H_2O from the coal surface because of pore increases during the throttling process. In Fig. 8(b), it is apparent that LCO_2 extracted some of the volatile products from the coal surface, which was accomplished by pore increases and bond weakening. This product included condensable coal tar (C_xH_y) and non-condensable gases such as CO [23]. This enhanced adsorption/desorption behavior of compressed CO_2 in coal is due to the high diffusivity, solubility, and plasticizing action into the coal surface.

Fig. 9 shows micrographs of (a) raw coal and (b) a coal particle sample after flash boiling at a decreasing pressure condition of 65/40 bar. These samples were compared at two magnification levels: ×700 and ×1200. As these images show, there are severe structural changes when raw coal undergoes the throttling process. Some of particles appear to break down into smaller particles, and numerous pores developed on the coal particles. Again, this may be due to evolution of the devolatilized/gasified gas from the surface and pore of coal particles. This finding is consistent with an increase in the Brunauer, Emmett and Teller (BET) surface area for coal dried with supercritical CO_2 [8]. The drying effect of supercritical CO_2 on the coal structures was examined. Fourier transform infrared (FT-IR) spectroscopy, BET surface area measurement, and solvent swelling were adopted to analyze the physical properties of the coal. The surface area and pore volume of coal dried with supercritical CO_2 are larger than those for thermally-dried coal. The CO_2-treated coal can uptake solvent rapidly into its structure. The supercritical CO_2 extraction of water from LRCs is considered an effective drying method for the preparation of activated coal in the combustion and liquefaction process.

The coal conversion was calculated by using the ash trace method. The composition results from proximate analysis are listed in Table 3, and are substituted into Eq. (1) for coal conversion. The coal conversion was 86.3% at the pressure condition of 65/40 bar. This result indicates the carbon conversion for coal samples experiencing the flash boiling condition of 65/40 bar. Both conversion data and microstructure changes support the coal devolatilization process at the flashing spray condition of LCO_2. A similar conversion was observed in the flash pyrolysis process when using the coal dried with supercritical CO_2. This phenomenon was hypothesized to increased fragmental radicals formed during the flash pyrolysis. This was caused by easier diffusion from the large pores

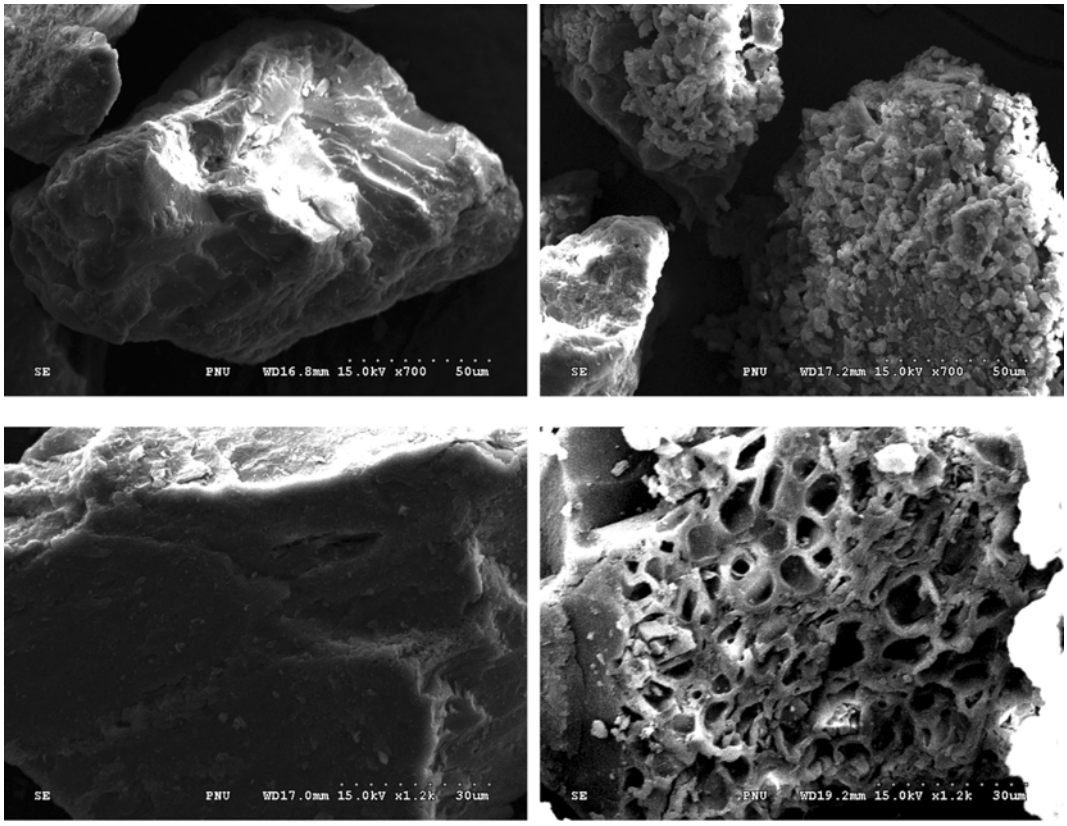

Fig. 9. Micrographs of coal particles at different magnification levels (×700 and ×1200): (a) Raw coal and (b) coal after flash boiling at pressure conditions of 65/40 bar.

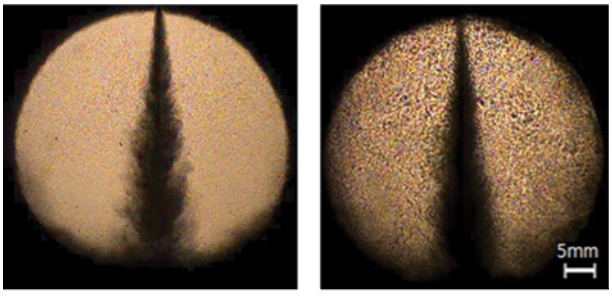

Fig. 10. Spray patterns of coal-LCO_2 slurry at the pressure condition of 65/40 bar at two different coal blending ratios of (a) 1.5 wt% and (b) 5 wt%.

of such coal [9,10]. However, no previous result has been reported on the flash devolatilization of coals during the throttling process across the nozzle.

Fig. 10 shows the spray patterns of coal-LCO_2 slurry at the pressure condition of 65/40 bar at two different coal blending ratio of (a) 1.5 wt% and (b) 5 wt%. There was no discernible difference in spray patterns, which were evaluated in terms of spray angle and penetration. However, a little higher contrast was observed with 5 wt% blending ratio. A blending ratio higher than 5 wt% was avoided as it could block the visualization by darkening an optical window more quickly.

3. Spray Patterns of Coal-water Slurry (CWS)

Fig. 11 compares spray patterns of different fluids at the same pressure condition of 65/40 bar. At the same nozzle length and diameter, the spray of H_2O is not fully developed, compared with that of LCO_2. The size of droplet ranges from 0.5 to 1 mm, which is much larger than the average size of a few tens of microns for droplets in LCO_2 spray. This is characteristic of a low Weber number condition, in which the liquid jet is not leaving the nozzle as atomized droplets. The Weber number has been useful in analyzing thin film flows and in the formation of droplets and bubbles. It is defined as the ratio of fluid inertia to the surface tension restraining the liquid, as written below:

$$We = \frac{\rho \cdot v^2 \cdot l}{\sigma} \quad (2)$$

where

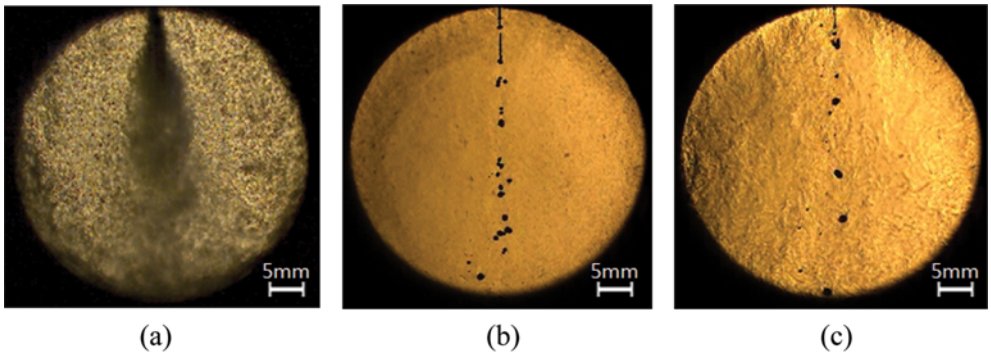

Fig. 11. Spray patterns of different fluids at the same pressure condition of 65/40 bar: (a) LCO_2, (b) H_2O, and (c) H_2O-coal slurry.

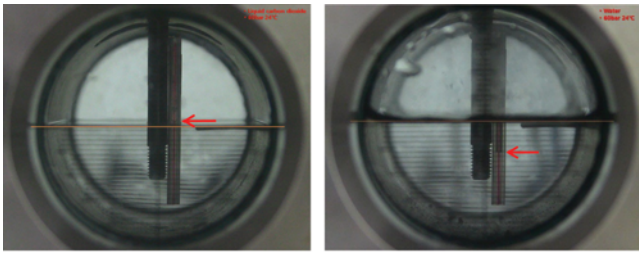

Fig. 12. Comparison of surface tension (i.e., a cohesive force) at the same pressure and temperature between two fluids: (a) LCO_2 and (b) H_2O.

ρ is the density of the fluid (kg/m^3)
v is its velocity (m/s)
l is its characteristic length, typically the droplet diameter (m), and
σ is the surface tension (N/m).

From this definition (Eq. (2)), weak atomization is expected because of low velocity and higher surface tension when the H_2O flows with high viscosity inside the nozzle. This breakup mode is similar to the Rayleigh-type breakup mode seen in the experiment of Liu and coworkers [15]. This was the main atomization zone of high-viscosity CWS. They also observed that a high-viscosity CWS jet continues to oscillate. For this reason, a surfactant was used to produce better atomization for the CWS [24]. Furthermore, a larger single droplet was observed for the coal slurry with H_2O. The droplet was entangled and grown near the nozzle. Once it reached the critical diameter of 5 mm, the droplet exited the nozzle. It is likely to experience more difficulty in leaving the nozzle due to a much lower velocity caused by the presence of the coal suspension in the flow.

Fig. 12 shows a comparison of the surface tension (i.e., cohesive force) of two fluids at the condition of 60 bar and 22 °C. The solid line represents the level of LCO_2 and H_2O that filled the upper chamber. The capillary tube was dipped into each fluid. The level of each fluid in the capillary tube represented how strong the cohesive force (surface tension) is as compared to the adhesive force between the fluid and the tube wall. The higher cohesive force lowers the fluid level in the capillary tube. The result shows that water has a much lower level than LCO_2. This indicates the higher cohesive force of water, which may provide the evidence for the

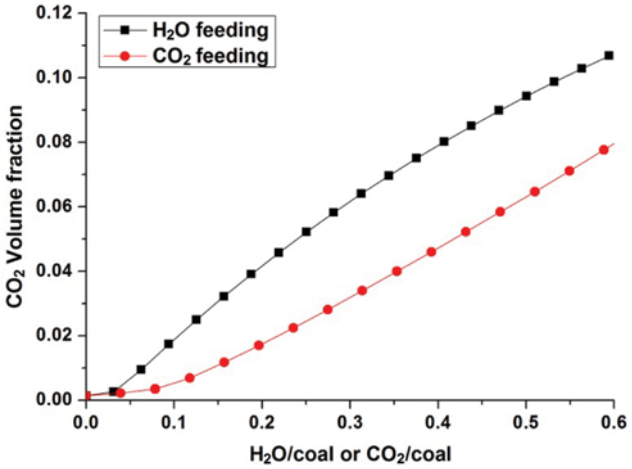

Fig. 13. Comparison of CO_2 emission between H_2O feeding and CO_2 feeding.

higher surface tension for water as discussed above.

The equilibrium calculation was simply made to quantify the reduction of CO_2 emission with transport medium of CO_2 against H_2O. The equilibrium solution was obtained by using the open source software, Cantera [25,26]. As shown in Fig. 13, the CO_2 emission with CO_2 feeding was compared against one with H_2O feeding on the same basis of feeding rate relative to coal. The result shows 50% reduction in CO_2 emission with CO_2 feeding at ratio of feeding agent to coal of 0.2. However, such degree of reduction becomes smaller (about 20%) as the ratio increases up to 0.6. This reduction may be due to Boudouard reaction where CO_2 is reacted with carbon to produce a CO gas.

CONCLUSION

We investigated the pressure effect on the flashing spray and devolatilization characteristics for LCO_2 and its mixture with coal. The results show that spray patterns changed significantly, from bowl spray to normal jet spray, with increased liquid flow rate as the upstream pressure increased. This difference was caused by the difference in the bursting degree of bubbles inside the nozzle, which is called internal flashing atomization. The absence of flashing spray at the pressure condition of 85/60 bar delivered coal particles more uniformly downstream across the chamber. The flash devolatilization process of coal occurs when coal particles are sprayed under the flashing boiling condition. At low Weber numbers in the spray condition of H_2O, the liquid jet is not leaving the nozzle properly, which is called the Rayleigh-type breakup mode.

ACKNOWLEDGEMENTS

This work was supported by a National Research Foundation of Korea (NRF) grant funded by the Korean government (MEST) (No. 2010-0019543). Some of the results are the outcome of another program (No. 2012R1A1A2002669), also supported by the NRF. Finally, the authors thank the Korean government (MKE) for financial support from the manpower program (No. 20144010200780).

REFERENCES

1. J. Dooher and J. Phillips, *Program on technology innovation: advanced concepts in slurry-fed low-rank coal gasification liquid CO_2/coal slurries and hot water drying*, EPRI Report, Dooher Institute (2006).
2. C. Botero, *The phase inversion-based coal-CO_2 slurry (PHICCOS) feeding system: design, coupled multiscale analysis, and technoeconomic assessment*, Ph.D. Dissertation, MIT (2014).
3. C. Botero, R. P. Field, H. J. Herzog and A. F. Ghoniem, *Energy Procedia*, **37**, 2212 (2013).
4. T. C. Lin, Y. J. Shen and M. R. Wang, *J. Aerosol. Sci.*, **61**, 27 (2013).
5. Y. Zeng and C. F. F. Lee, *Combustion Sci. Technol.*, **169**, 45 (2001).
6. Y. H. Liu, G. Calvert, C. Hare, M. Ghadiri and S. Matsusaka, *J. Aerosol. Sci.*, **48**, 1 (2012).
7. Y. H. Liu, H. Maruyama and S. Matsusaka, *Adv. Powder Technol.*, **21**, 652 (2010).
8. Y. Iwai, T. Murozono, Y. Koujina, Y. Arai and K. Sakanishi, *J. Supercrit. Fluids*, **18**, 73 (2000).
9. Y. Iwai, Y. Koujina, Y. Arai, I. Watanabe, I. Mochida and K. Sakanishi, *J. Supercrit. Fluids*, **23**, 251 (2002).
10. F. P. Lucien and N. R. Foster, *J. Supercrit. Fluids*, **17**, 111 (2000).
11. A. R. Berens, G. S. Huvard, R. W. Korsmeyer and F. W. Kunig, *J. Appl. Polym. Sci.*, **46**, 231 (2003).
12. G. A. Nunez, M. I. Briceno, D. D. Joseph and T. Asa, *Colloidal coal in water suspensions*, Available Online (2005).
13. S. Y. Son and K. D. Kihm, *Atomization Sprays*, **8**, 503 (1998).
14. Z. Farago and N. Chigier, *Atomization Sprays*, **2**, 137 (1992).
15. A. Dechelette, O. Campanella, C. Corvalan and P. E. Sojka, *Chem. Eng. Sci.*, **66**, 6367 (2011).
16. H. Zhao, H. F. Liu, J. L. Xu, W. F. Li and W. Cheng, *Chem. Eng. Sci.*, **78**, 63 (2012).
17. R. D. Reitz, *Aerosol Sci. Technol.*, **12**, 561 (1990).
18. J. Senda, Y. Hojyo and H. Fujimoto, *JSAE Rev.*, **15**, 291 (1994).
19. S. Park and S. Y Lee, *Atomization Sprays*, **4**, 159 (1994).
20. J. Xiao, X. Qiao, Z. Huang and J. Fang, *Chinese Sci. Bulletin*, **49**, 1195 (2004).
21. C. Y. Wen and T. Z. Chaung, *Ind. Eng. Chem. Process Des. Dev.*, **18**, 684 (1979).
22. R. Govind and J. Shah, *AIChE J.*, **30**, 79 (1984).
23. *Coal liquefaction*, Available Online, http://en.wikipedia.org/wiki/Coal_liquefaction# cite_note-lee3-6.
24. R. Xu, W. Zhuang, Q. He, J. Cai, B. Hu and J. Shen, *AIChE J.*, **55**, 2461 (2009).
25. P. Baggio, M. Baratieri, L. Fiori, M. Grigiante, D. Avi and P. Tosi, *Energy Convers. Manage.*, **50**, 1426 (2009).
26. A. Melgar, J. F. Perez, H. Laget and A. Horillo, *Energy Convers. Manage.*, **48**, 59 (2007).